Photoionization loss in simultaneous magneto-optical trapping of Rb and Sr

Takatoshi Aoki,[*] Yuki Yamanaka, Makoto Takeuchi, and Yoshio Torii

Institute of Physics, Graduate School of Arts and Sciences, University of Tokyo, Tokyo 153-8902, Japan

Yasuhiro Sakemi

Cyclotron and Radioisotope Center, Tohoku University, Sendai 980-8578, Japan

We demonstrate the simultaneous magneto-optical trapping (MOT) of Rb and Sr and examine the characteristic loss of Rb in the MOT due to photoionization by the cooling laser for Sr. The photoionization cross section of Rb in the $5P_{3/2}$ state at 461 nm is determined to be $1.4(1) \times 10^{-17}$ cm^2. It is important to consider this loss rate to realize a sufficiently large number of trapped Rb atoms to achieve a quantum degenerate mixture of Rb and Sr.

I. INTRODUCTION

During the last decade, quantum degenerate mixtures of different atomic species have been investigated by many researchers [1–6]. These systems have included research of Bose-Fermi mixtures [7], the Fulde-Ferrell-Larkin-Ovchinnikov (FFLO) state near the BCS–Bose-Einstein-condensate (BEC) crossover with different masses [8], self-trapping in optical lattices [9], and the heteronuclear Efimov state [10]. The heteronuclear molecule comprised of two different atomic species in the rovibrational ground state has an electric dipole moment, and ultracold RbK molecules in the rovibrational ground state have been realized using stimulated Raman adiabatic passage (STIRAP) [11]. Ultracold polar molecules enable us to study new quantum phases [12] and quantum logic gates [13].

Recently, polar molecules comprised of alkali-metal and alkaline-earth-metal (or rare-earth-metal) atoms have come under increasing scrutiny because such polar molecules have an electron spin in the rovibrational ground state in addition to an electric dipole moment, which offers the chance to study new quantum phases of the lattice spin model [14], precise measurement [15], and fundamental physics [16]. One such example is YbRb, whose molecules in the excited states are generated by two-photon photoassociation in a mixture of ultracold Rb and Yb [17]. Recently, quantum degenerate mixtures of LiYb have been reported [18], but the LiYb molecule has a relatively small electric dipole moment (0.02–0.15 Debye) [19]. In contrast, the RbSr molecule is expected to have a relatively large electric dipole moment (1.4 Debye) [20]. Furthermore, the theoretically predicted heteronuclear Feshbach resonances of RbSr [21] indicate that it is possible to associate ultracold Rb and Sr atoms to produce the RbSr molecule. Because techniques for laser cooling of Rb and Sr are well established, quantum degeneracy of Sr has been achieved by several groups [22]. However, simultaneous laser cooling of Rb and Sr has not yet been reported.

In this work we demonstrate simultaneous magneto-optical trapping (MOT) of Rb and Sr. We observe the characteristic loss of Rb in the MOT, which can be understood as photoionization due to the 461-nm cooling beam for the Sr atoms. The

loss rate was measured by changing the intensity of the 461-nm laser beam, and the photoionization cross section of Rb in the $5P_{3/2}$ state was determined. We found that simultaneous MOT of Rb and Sr is possible with a cooling beam for Sr at the saturation intensity.

II. PHOTOIONIZATION IN SIMULTANEOUS MOT

Photoionization is the ionization of a neutral atom due to an atom-light interaction. Figure 1 shows the energy diagrams and laser transitions for simultaneous laser cooling of Rb and Sr. The wavelengths of the cooling transitions are 461 and 780 nm for Sr and Rb, respectively. The 780-nm laser does not ionize Sr in the excited state $^1P_1$ because photoionization from this state requires a photon energy of 415 nm. However, the wavelength from the Rb $5P_{3/2}$ state to the ionization threshold is 479 nm, and so the 461-nm laser can ionize Rb atoms in the $5P_{3/2}$ state. This photoionization would result in trap loss in simultaneous MOT of Rb and Sr. For previously reported alkali-metal–alkali-metal mixtures, i.e., Li-Na [1], Li-K [2], Li-Rb [3], K-Na [4], K-Rb [5], Rb-Cs [6], and Yb-Li [18], photoionization due to the cooling laser did not occur because the photon energies of the cooling beams were smaller than the photoionization energies.

The loss rate R due to photoionization is given by [23,24],

$$R = \Phi f \sigma, \tag{1}$$

where $\Phi = I/h\nu$ is the photon flux, I is the intensity of the photoionization laser beam, h is the Planck constant, ν is the optical frequency of the photoionization laser beam, f is the population fraction of the excited state, i.e., the $5P_{3/2}$ state of Rb, and σ is the photoionization cross section. Taking into account the photoionization loss rate, the rate equation for the number of Rb atoms in the MOT is written as [25]

$$\frac{dN_{\text{Rb}}(t)}{dt} = \Gamma - \frac{1}{\tau}N_{\text{Rb}}(t) - B - RN_{\text{Rb}}(t), \tag{2}$$

where the $N_{\text{Rb}}(t)$ is the number of trapped Rb atoms as a function of time, Γ is the loading rate of the Rb MOT, and τ is the decay time constant due to background gas collisions. The loss coefficient $B = \beta_{\text{RbRb}} \int n_{\text{Rb}}^2(r)d^3r + \beta_{\text{RbSr}} \int n_{\text{Rb}}(r)n_{\text{Sr}}(r)d^3r$ is due to light-assisted collisions, where β_{RbRb} and β_{RbSr} are the light-assisted collision coefficients between the Rb atoms and between the Rb and Sr atoms, respectively, and

—————————
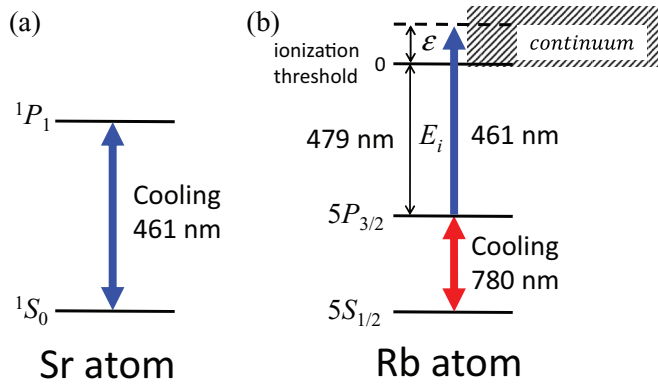[*]aoki@phys.c.u-tokyo.ac.jp

FIG. 1. (Color online) Energy diagrams and relevant transitions of (a) Sr and (b) Rb. The ionization energy E_i from the $5P_{3/2}$ state of Rb corresponds to a wavelength of 479 nm. Excess energy ϵ is converted into the kinetic energy of the ionized Rb atom and the electron.

$n_{\mathrm{Rb}}(r)$ and $n_{\mathrm{Sr}}(r)$ are the respective spatial densities of Rb and Sr. Because light-assisted collisions between the Rb and Sr atoms were not observed, as described in Sec. IV, and the density of the trapped Rb can be assumed to be constant in a usual MOT experiment [26], B can be approximated as $B \simeq \beta_{\mathrm{RbRb}} n_{\mathrm{Rb}} N_{\mathrm{Rb}}(t)$, where n_{Rb} is a constant density. Then, Eq. (2) is written as

$$\frac{dN_{\mathrm{Rb}}(t)}{dt} = \Gamma - \frac{1}{\tau'} N_{\mathrm{Rb}}(t) - R N_{\mathrm{Rb}}(t), \qquad (3)$$

where $1/\tau' \equiv 1/\tau + \beta_{\mathrm{RbRb}} n_{\mathrm{Rb}}$. The solution to Eq. (3), when $R\ (\neq 0)$ is introduced at time $t = 0$, is written as

$$N(t) = N_\infty + (N_0 - N_\infty) \exp(-R't), \qquad (4)$$

where $R' \equiv R + 1/\tau'$, N_0 is the steady-state atom number for the rate equation with $R = 0$, and N_∞ is that for an arbitrary R. Using this solution, measurement of the decay of the number of Rb atoms in the MOT allows us to determine the photoionization rate R and the photoionization cross section σ of Rb in the $5P_{3/2}$ state at 461 nm.

III. SIMULTANEOUS MOT

Our laser system and frequency locking scheme for cooling the Sr atoms are similar to those described in Ref. [27]. Briefly, a laser beam with a wavelength of 922 nm from an extended cavity diode laser (ECDL) was amplified by a tapered amplifier (TA) up to 900 mW. This laser beam enters a frequency doubling cavity, which generates a 461-nm laser beam with a power of 175 mW. The frequency was stabilized by using frequency modulation spectroscopy with a Sr hollow-cathode lamp. The repumping beam, also generated by frequency doubling, has a wavelength of 497 nm and is resonant with the transition between $5s5p\ ^3P_2$ and $5s5d\ ^3D_2$ states.

For cooling the Rb, we used a commercially available extended cavity tapered laser (ECTL), and an ECDL was used for the repumping. The frequencies of these laser beams were stabilized by the polarization spectroscopy of a Rb cell [28].

Figure 2(a) shows the vacuum system, which was comprised of ovens, Zeeman slowers, and a main chamber with a design similar to that in Ref. [29]. The vapor pressures of Rb
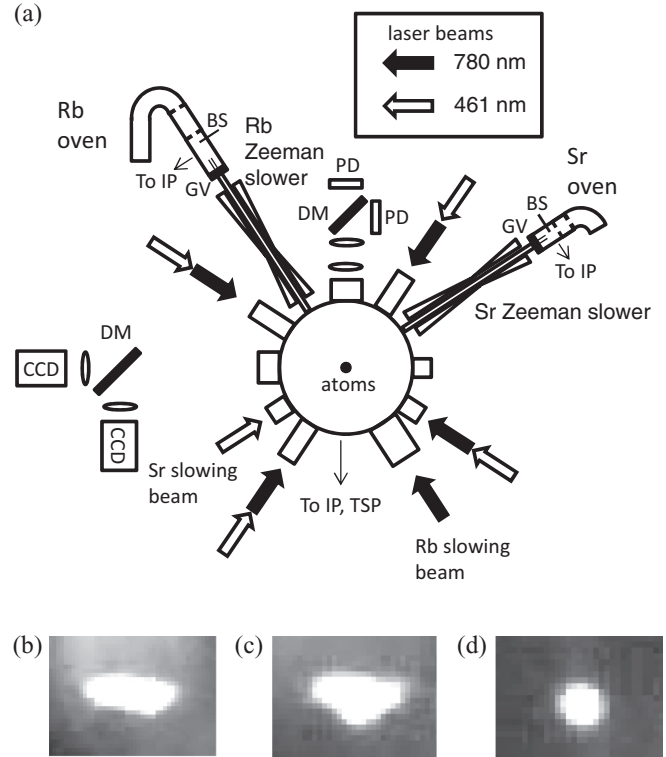

FIG. 2. (a) Schematic diagram of the experimental apparatus. IP: ion pump; TSP: Ti-sublimation pump (these vacuum pumps are not shown); BS: beam shutter; GV: gate valve; DM: dichroic mirror; and PD: photodetector. The 780- and 461-nm laser beams are shown by the black and white arrows, respectively. (Trapping beams propagating perpendicular to this diagram are not shown.) Fluorescence images of the trapped (b) Sr, (c) Sr and Rb, and (d) Rb atoms. In (c), the trapped clouds of Rb and Sr are spatially overlapped. The field of view is $7.5 \times 5.6\ \mathrm{mm}^2$.

and Sr are quite different: a pressure of 1×10^{-4} Torr inside the oven is achieved at about $100\,^\circ\mathrm{C}$ for Rb but at $400\,^\circ\mathrm{C}$ for Sr. We therefore prepared separate ovens and Zeeman slowers for each atomic species. The Rb (Sr) atomic beam was extracted from the Rb (Sr) oven and passed through the oven chamber, whose background pressure was 10^{-8} Torr, whereas the background pressure of the main chamber was kept below 2×10^{-11} Torr by using a 75-L/s ion pump and a Ti-sublimation pump.

The Rb atomic beam was first extracted from the Rb oven and decelerated by the Rb Zeeman slower; the Sr atomic beam is decelerated by the Sr Zeeman slower. The Zeeman slowers have zero-crossing designs, and the magnetic field at the exit of the slower is 100 G (600 G) for Rb (Sr). The trapping beam for the Rb (Sr) with a wavelength of 780 nm (461 nm) was split into three beams by waveplates and polarization beam splitters. These beams are overlapped by dichroic mirrors and pass through the achromatic quarter waveplates, creating circularly polarized beams. The repumping beam for Rb is overlapped with the Rb slowing beam, whereas the repumping beam for Sr is overlapped with one of Sr trapping beams. The decelerated atomic beams enter the main chamber and reach the intersection of the three orthogonal trapping beams for Rb and Sr. The Rb and Sr atoms are then simultaneously trapped.
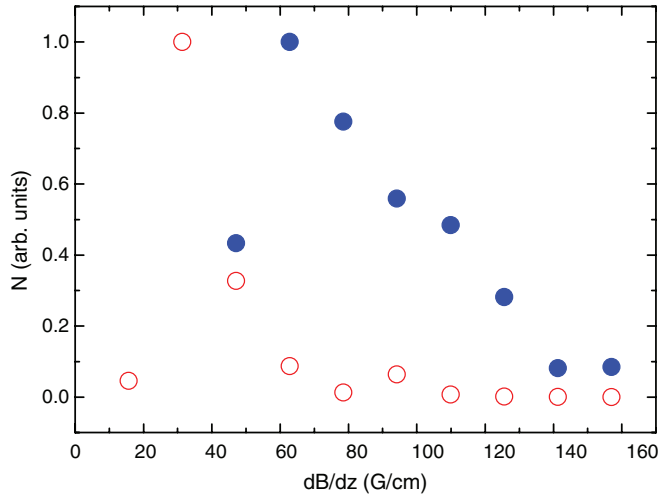
FIG. 3. (Color online) Number of trapped Rb and Sr atoms versus the magnetic field gradient. The solid circles denote Sr, and the open circles denote Rb. The numbers of trapped atoms are normalized to the maximum values.

Figures 2(b)–2(d) show fluorescence images of the trapped clouds in the MOT taken by a charge-coupled device (CCD) camera. The trapped Rb and Sr clouds are spatially overlapped in the image. The power and diameter of each trapping beam was 15 mW (10 mW) and 34 mm (16 mm), respectively, for Rb (Sr), and the power of the slowing and repumping beams were 25 mW (2.3 mW) and 20 mW (150 μW) for Rb (Sr), respectively. A 20-MHz (40-MHz) detuning was used for Rb (Sr). To obtain an image of both Rb and Sr, we chose a magnetic field gradient along the axial direction of 90 G/cm to reduce the size of the trapped Rb cloud to that comparable with the Sr cloud. The fluorescence from the Rb atoms is stronger than that from the Sr atoms, and the CCD camera has a higher sensitivity at 780 nm than at 461 nm. Thus, the fluorescence signal on the CCD camera from the trapped Rb atoms saturates easily. To reduce the Rb signal, the fluorescence from both species was passed through a dichroic mirror that is transparent at 461 nm but reduces the intensity of 780-nm light. This allowed the fluorescence from both the Rb and Sr to be simultaneously detected as shown in Figs. 2(b)–2(d).

The dependence of the number of trapped atoms on the magnetic field gradient is shown in Fig. 3. The number of trapped Rb atoms is maximized (1×10^{10}) at a field gradient of 30 G/cm, whereas the number of Sr atoms is maximized (1×10^6) at 60 G/cm. The difference in the two magnetic field gradients stems from the difference in the natural line widths (6 MHz for Rb and 32 MHz for Sr).

IV. MEASUREMENT OF THE PHOTOIONIZATION RATE

Understanding the loss is important for achieving a large number of trapped atoms. Light-assisted collisions have a large effect on conventional alkali-atom trapping experiments. However, we did not observe this type of loss in the simultaneous MOT under our experimental conditions. Instead, when the trapped Rb atoms were irradiated by the 461-nm laser beams, the number of Rb atoms decreased due to photoionization.
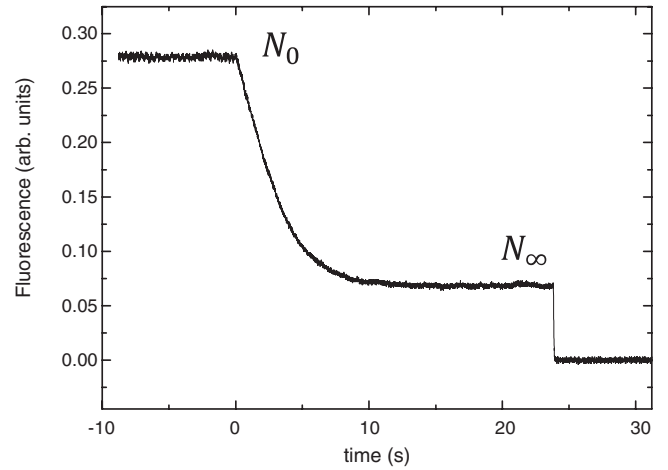

FIG. 4. Typical decay signal of Rb atoms in the MOT. The 461-nm laser beam is turned on at $t = 0$. The intensity of the 461-nm beam was 307 mW/cm^2, which corresponds to an intensity 7.3 times the saturation intensity for the cooling transition of Sr.

To measure the photoionization cross section, the trapped Rb cloud is irradiated by the 461-nm laser beam at various intensities. The counterpropagating beam, which is generated by a mirror, also interacts with the atoms to double the intensity of the photoionization beam. We first load a Rb MOT with a trapping beam diameter of 17 mm, and the fluorescence signal from the trapped Rb atoms is detected by a photodetector. The number of atoms in the MOT exhibits a nearly simple exponential growth with a time constant of 5 s, indicating that $1/\tau' \simeq 0.2$. After the the number of trapped atoms saturates, the Rb cloud is irradiated by the 461-nm beam. Figure 4 shows the typical decay due to photoionization of the number of trapped Rb atoms. The intensity of the 8-mm photoionization beam was 307 mW/cm^2. The number of Rb atoms decays after the 461-nm beam is turned on, and after the trapping beams are switched off at 24 s, the signal returns to the background level of the photodetector.

Figure 4 indicates that trapped atoms remain after the photoionization-induced decay. The number of trapped atoms is determined by the balance between the Rb loading rate from the slowed atomic beam and the photoionization loss rate [Eq. (2)]. If we choose a beam intensity that is lower than the saturation intensity $I_s = 42$ mW/cm^2, a Rb atom loss of only 10–20% is seen. A typical trapping experiment requires the intensity of the MOT beams to be close to that of I_s, and thus this result strongly supports the possibility of simultaneous MOT of Rb and Sr with a large number of atoms.

The decay constant R' is evaluated by fitting Eq. (4) to the decay curve. Then, we obtained R by subtracting $1/\tau'$ from R'. According to Eq. (1), R is a function of the intensity I, and to estimate the photoionization cross section, we measured R by changing I as shown in Fig. 5. As expected, R is proportional to I. By fitting Eq. (1) to the experimental data and using $f = 0.19$, the photoionization cross section of Rb in the $5P_{3/2}$ state is given as $(1.4 \pm 0.1) \times 10^{-17}$ cm^2. The value of f is calculated from the detuning of the Rb MOT beam (-16 MHz) and the intensity $I_{\mathrm{Rb}} = 12\, I_{\mathrm{Rb,s}}$, where I_{Rb} is the intensity of the Rb MOT beam, and $I_{\mathrm{Rb,s}} = 1.6$ mW/cm^2 is the saturation intensity of the cooling transition for Rb. The uncertainty in
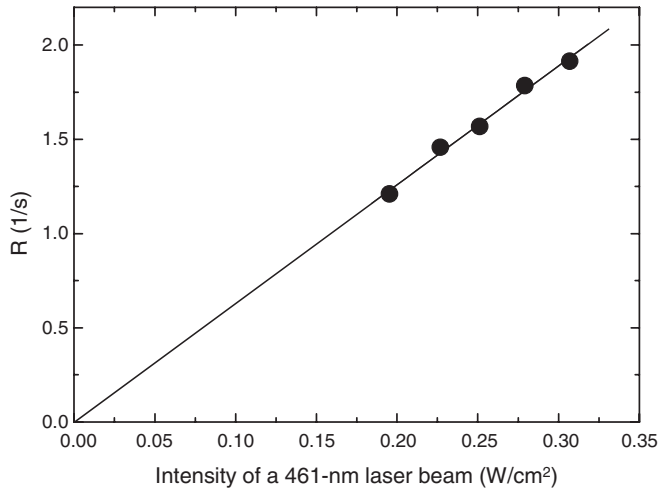
FIG. 5. Decay constant versus the intensity of the 461-nm beam. The solid circles are the measured values, and the solid line is a theoretical fit to the data.

the cross section comes mainly from the uncertainty in the determination of the population f in the $5P_{3/2}$ state.

The photoionization cross section is determined by the matrix element of the transition dipole moment between the initial atomic state and the continuum state above the ionization threshold, and thus it depends on the excess energy ϵ in Fig. 1(b) (see Ref. [30]). The photoionization cross section of the Rb atom in the $5P_{3/2}$ state has been investigated by several other groups for different wavelengths. Aymar *et al.* [31] calculated the cross section theoretically and found cross sections of 1.19, 1.22, and 1.30×10^{-17} cm^2 at 440 nm, and 1.25, 1.30, and 1.40×10^{-17} cm^2 at the 479-nm threshold. Dinneen *et al.* [23] measured the cross section to be 1.25(11) and $1.36(12) \times 10^{-17}$ cm^2 at 407 and 413 nm using MOT of Rb. A value of $1.48(22) \times 10^{-17}$ cm^2 at 476.5 nm was measured by Gabbanini *et al.* [25], and a cross section of 0.54(12) and $1.34(16) \times 10^{-17}$ cm^2 at 296 nm using a pulse laser and at 421 nm using a continuous-wave laser were found by Ciampini *et al.* [32]. Work by Nadeem *et al.* [33] determined cross sections of 1.25, 1.26, 1.36, 1.5, and 1.88×10^{-17} cm^2 at 425, 440, 460, 476.5, and 479 nm using a pulsed laser and a

Rb heat pipe with an Ar buffer gas. The overall uncertainty in the cross section by Nadeem *et al.* is 16%, and a cross section at 460 nm of $1.36(21) \times 10^{-17}$ cm^2 was given in Ref. [33]. Our value of $1.4(1) \times 10^{-17}$ cm^2 at 460.862 nm is in good agreement with this value.

V. CONCLUSION

We have demonstrated the simultaneous MOT of Rb and Sr. Both species have different optimum values of the magnetic field gradient that maximize the number of trapped atoms. Loss due to light-assisted collisions between Rb and Sr was not observed under our experimental conditions, but the cooling beam for Sr causes photoionization-induced loss of Rb in the excited $5P_{3/2}$ state. This had not previously been observed for other alkali-metal and alkaline-earth-metal (two-electron) atom mixtures.

In spite of the photoionization loss, we realized simultaneous MOT of Rb and Sr under the typical intensity of the 461-nm beam. The measurement of the photoionization loss rate as a function of the beam intensity gave the photoionization cross section at 460.862 nm as $1.4(1) \times 10^{-17}$ cm^2. We believe that this value is useful for optimizing the numbers of trapped Rb and Sr atoms in a simultaneous trapping experiment.

Currently, we are preparing a laser system for cooling Sr using the 689-nm narrow line transition. The next step is to cool Sr atoms below 1 μK and to load the Rb and Sr into an optical dipole trap. A quantum degenerate mixture of Rb and Sr will realize ultracold polar molecules with electron spins and promote research of new quantum phases.

[1] Z. Hadzibabic, C. A. Stan, K. Dieckmann, S. Gupta, M. W. Zwierlein, A. Gorlitz, and W. Ketterle, Phys. Rev. Lett. **88**, 160401 (2002).

[2] M. Taglieber, A.-C. Voigt, T. Aoki, T. W. Hänsch, and K. Dieckmann, Phys. Rev. Lett. **100**, 010401 (2008); F. M. Spiegelhalder, A. Trenkwalder, D. Naik, G. Kerner, E. Wille, G. Hendl, F. Schreck, and R. Grimm, Phys. Rev. A **81**, 043637 (2010).

[3] C. Silber, S. Gunther, C. Marzok, B. Deh, P. W. Courteille, and C. Zimmermann, Phys. Rev. Lett. **95**, 170408 (2005).

[4] J. W. Park, C. H. Wu, I. Santiago, T. G. Tiecke, S. Will, P. Ahmadi, and M. W. Zwierlein, Phys. Rev. A **85**, 051602(R) (2012).

[5] G. Roati, F. Riboli, G. Modugno, and M. Inguscio, Phys. Rev. Lett. **89**, 150403 (2002); G. Modugno, M. Modugno, F. Riboli, G. Roati, and M. Inguscio, *ibid.* **89**, 190404 (2002); J. Goldwin, S. Inouye, M. L. Olsen, B. Newman, B. D. DePaola, and D. S. Jin, Phys. Rev. A **70**, 021601(R) (2004); C. Ospelkaus, S. Ospelkaus, K. Sengstock, and K. Bongs, Phys. Rev. Lett. **96**, 020401 (2006); K. Günter, T. Stöferle, H. Moritz, M. Köhl, and T. Esslinger, *ibid.* **96**, 180402 (2006); S. Aubin *et al.*, Nat. Phys. **2**, 384 (2006).

[6] A. D. Lercher *et al.*, Eur. Phys. J. D **65**, 3 (2011).

[7] S. Ospelkaus, C. Ospelkaus, O. Wille, M. Succo, P. Ernst, K. Sengstock, and K. Bongs, Phys. Rev. Lett. **96**, 180403 (2006).

[8] A. Feiguin, F. Heidrich-Meisner, G. Orso, and W. Zwerger, Lect. Notes Phys. **836**, 503 (2012).

[9] T. Best, S. Will, U. Schneider, L. Hackermuller, D. vanOosten, I. Bloch, and D. S. Luhmann, Phys. Rev. Lett. **102**, 030408 (2009).

[10] G. Barontini, C. Weber, F. Rabatti, J. Catani, G. Thalhammer, M. Inguscio, and F. Minardi, Phys. Rev. Lett. **103**, 043201 (2009).

[11] K.-K. Ni *et al.*, Science **322**, 231 (2008).

[12] H. P. Buchler, E. Demler, M. Lukin, A. Micheli, N. Prokofev, G. Pupillo, and P. Zoller, Phys. Rev. Lett. **98**, 060404 (2007).

[13] D. DeMille, Phys. Rev. Lett. **88**, 067901 (2002).

[14] A. Micheli, G. K. Brennen, and P. Zoller, Nat. Phys. **2**, 341 (2006).

[15] M. Kajita, G. Gopakumar, M. Abe, and M. Hada, Phys. Rev. A **84**, 022507 (2011).

[16] T. Aoki *et al.*, in *Proceedings of the 5th International Workshop on Fundamental Physics Using Atoms 2011, Okayama, 2011*, edited by N. Sasao (Okayama University, Okayama, Japan, 2011), p. 118.

[17] N. Nemitz, F. Baumer, F. Münchow, S. Tassy, and A. Görlitz, Phys. Rev. A **79**, 061403 (2009).

[18] H. Hara, Y. Takasu, Y. Yamaoka, J. M. Doyle, and Y. Takahashi, Phys. Rev. Lett. **106**, 205304 (2011); A. H. Hansen, A. Khramov, W. H. Dowd, A. O. Jamison, V. V. Ivanov, and S. Gupta, Phys. Rev. A **84**, 011606(R) (2011).

[19] P. Zhang, H. R. Sadeghpour, and A. Dalgarno, J. Chem. Phys. **133**, 044306 (2010); G. Gopakumar, M. Abe, B. P. Das, M. Hada, and K. Hirao, *ibid.* **133**, 124317 (2010); S. Kotochigova,

[20] R. Guérout, M. Aymar, and O. Dulieu, Phys. Rev. A **82**, 042508 (2010).

[21] P. S. Żuchowski, J. Aldegunde, and J. M. Hutson, Phys. Rev. Lett. **105**, 153201 (2010).

[22] S. Stellmer, M. K. Tey, B. Huang, R. Grimm, and F. Schreck, Phys. Rev. Lett. **103**, 200401 (2009); Y. N. Martinez de Escobar, P. G. Mickelson, M. Yan, B. J. DeSalvo, S. B. Nagel, and T. C. Killian, *ibid.* **103**, 200402 (2009).

[23] T. P. Dinneen, C. D. Wallace, K.-Y. N. Tan, and P. L. Gould, Optics Lett. **17**, 1706 (1992).

[24] F. Henkel, M. Krug, J. Hofmann, W. Rosenfeld, M. Weber, and H. Weinfurter, Phys. Rev. Lett. **105**, 253001 (2010).

[25] C. Gabbanini, S. Gozzini, and A. Lucchesini, Opt. Comm. **141**, 25 (1997).

[26] D. Hoffmann, P. Feng, R. S. Williamson, III, and T. Walker, Phys. Rev. Lett. **69**, 753 (1992).

[27] T. Aoki *et al.*, J. Phys. Soc. Jpn. **81**, 034401 (2012).

[28] Y. Torii, H. Tashiro, N. Ohtsubo, and T. Aoki, Phys. Rev. A **86**, 033805 (2012).

[29] E. W. Streed *et al.*, Rev. Sci. Instrum. **77**, 023106 (2006).

[30] A. L. Stewart, Adv. At. Mol. Phys. **3**, 1 (1967).

[31] M. Aymar, O. Robaux, and S. Wane, J. Phys. B: At. Mol. Phys. **17**, 993 (1984).

[32] D. Ciampini, M. Anderlini, J. H. Muller, F. Fuso, O. Morsch, J. W. Thomsen, and E. Arimondo, Phys. Rev. A **66**, 043409 (2002).

[33] A. Nadeem and S. U. Haq, Phys. Rev. A **83**, 063404 (2011).